

# ChemComm

Accepted Manuscript



This article can be cited before page numbers have been issued, to do this please use: X. Tian, Y. Zhu, Q. Zhang, R. Zhang, J. Wu and Y. Tian, *Chem. Commun.*, 2017, DOI: 10.1039/C7CC03640J.



This is an Accepted Manuscript, which has been through the Royal Society of Chemistry peer review process and has been accepted for publication.

Accepted Manuscripts are published online shortly after acceptance, before technical editing, formatting and proof reading. Using this free service, authors can make their results available to the community, in citable form, before we publish the edited article. We will replace this Accepted Manuscript with the edited and formatted Advance Article as soon as it is available.

You can find more information about Accepted Manuscripts in the [author guidelines](#).

Please note that technical editing may introduce minor changes to the text and/or graphics, which may alter content. The journal's standard [Terms & Conditions](#) and the ethical guidelines, outlined in our [author and reviewer resource centre](#), still apply. In no event shall the Royal Society of Chemistry be held responsible for any errors or omissions in this Accepted Manuscript or any consequences arising from the use of any information it contains.



Journal Name

COMMUNICATION

## Halides Tuning Subcellular-Targeting in Two-Photon Emissive Complexes via Different Uptake Mechanisms

Received 00th January 20xx,  
Accepted 00th January 20xx

Xiaohe Tian,<sup>†[a,b]</sup> Yingzhong Zhu,<sup>‡[b]</sup> Qiong Zhang,<sup>[b]</sup> Ruilong Zhang,<sup>\*,[b]</sup> Jieying Wu,<sup>[b]</sup> and Yupeng Tian<sup>\*,[b,c]</sup>

DOI: 10.1039/x0xx00000x  
www.rsc.org/

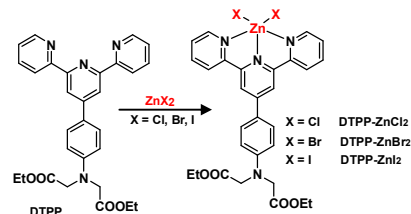
**We reported a simple and universal strategy by tuning halides (Cl, Br and I) in terpyridine-Zn(II) complexes to achieve different subcellular organelles targeting (nucleolus, nucleus and intracellular membrane system, respectively) via different cellular uptake mechanisms, resulting from halides triggering different polymorphies of these complexes.**

Nucleolus, nucleus, endoplasmic reticulum (ER) and other subcellular organelles are of universal interesting, as each subcellular compartment plays a key role in cell dividing, protein translation/transportation and otherwise.<sup>[1]</sup> Direct *in cellulo* visualization of these subcellular structures by the aid of fluorescent probes is very convenient as a powerful research method.<sup>[2-5]</sup> Within numerous fluorescent probes reported, we can change the location of fluorophores in living cells through the alteration of the targeting moieties, such as triphenylphosphonium could accumulate in mitochondria,<sup>[6-8]</sup> and morpholine could specially target acidic lysosomes.<sup>[9-11]</sup> However, such methods were time consuming and costly, and brought obstacles for further modification. Consequently, seeking a simple way to tune localizations intracellularly through the functionalization of fluorescent dyes is urgently required.

Metal-organic coordination is a widely used method to assign advantages to organic compound by the introductions of metal ions and counter-anions, including tunable properties and fluorescent enhancement.<sup>[12-14]</sup> In general, lanthanide ions (e.g. Eu(III) and Tb(III)),<sup>[15-17]</sup> group VIII elements ions (e.g. Ir(III), Ru(II) and Pt(II))<sup>[18-20]</sup> and other transition metal ions with  $d^0$ ,  $d^5$  and  $d^{10}$  electronic conformations<sup>[21-23]</sup> were usually applied in preparing coordinations with strong one- and two-photon fluorescence. Whereas most of these ions were not essential elements with relatively high toxicity, which would bring out large invasive effects and unexpected reactions in biological applications.<sup>[24, 25]</sup> To avoid these interferences, an essential

element ion, Zn(II) with  $d^{10}$  electronic configuration, was usually used to synthesize metal-organic complexes with low toxicities and strong emissions.<sup>[26-29]</sup> In present work, we reported that three terpyridine-ZnX<sub>2</sub> (X = Cl, Br and I) complexes can localize in distinct subcellular organelles *via* different cell entry mechanisms, achieving to visualize subcellular organelles simply.

Firstly, the ligand, diethyl 3-(4-([2,2':6',2''-terpyridin]-4'-yl)phenyl)pentanedioate (DTPP) and its three complexes DTTP-ZnCl<sub>2</sub>, DTTP-ZnBr<sub>2</sub> and DTTP-ZnI<sub>2</sub> (Scheme 1 and S1) have been synthesized, and characterized by <sup>1</sup>H NMR, <sup>13</sup>C NMR, MS and single-crystal XRD (Fig. S1-S7). Subsequently, their fluorescent properties have been investigated in Fig. 1. With the excitation at 385 nm, DTTP exhibited strong fluorescence at 480 nm. Different from the ligand DTTP, its three complexes underwent a redshift with the emission at around 540 nm, since the ligand binding to Zn(II) led to more extensive  $\pi$ -conjugated system and stronger intramolecular charge transfer, which were certified by computer-aided calculations (Fig. S8). In the two-photon fluorescence studies, it was found that the ligand DTTP could not emit two-photon fluorescence. Interestingly, after coordinating with Zn(II) halides, the two-photon emissions of the three complexes were apparently enhanced than that of DTTP as the reasons pointed above<sup>[30]</sup>. It should be noted that ligand DTTP without two-photon emission can be effectively avoid the interference from the disassociation of complexes under two-photon fluorescent imaging. On the basis of the optical spectra of three halides complexes, we selected 850 nm as excitation wavelength, and 550 - 600 nm as collected range (Fig. S9) for two-photon biological imaging after evaluating their cytotoxicity (Fig. S10, MTT assay).



<sup>a</sup> School of Life Science, Anhui University, Hefei 230039, P. R. China

<sup>b</sup> Department of Chemistry, Key Laboratory of Functional Inorganic Material Chemistry of Anhui Province, Anhui University, Hefei 230039, P. R. China

<sup>c</sup> State Key Laboratory of Coordination Chemistry, Nanjing University, Nanjing 210093, P. R. China

\* Correspondence: E-mail: xiaohe.t@ahu.edu.cn; yptian@ahu.edu.cn

† These authors contributed equally to this work.

Scheme 1. The structures of ligand **DTPP** and its three zinc halide complexes **DTPP-ZnX<sub>2</sub>** ( $X = \text{Cl}, \text{Br}$  and  $\text{I}$ ).

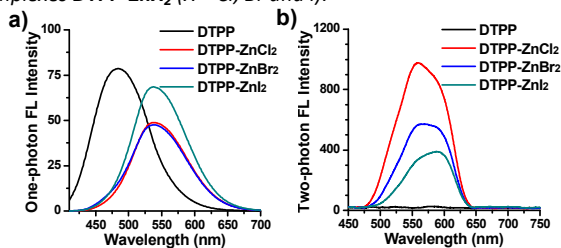


Fig. 1 One- (a) and two-photon excited at 850 nm (b) fluorescence spectra of **DTTP**, **DTTP-ZnCl<sub>2</sub>**, **DTTP-ZnBr<sub>2</sub>** and **DTTP-ZnI<sub>2</sub>**.

Subsequently, live cells staining using the three complexes were performed. HepG2 cells (human liver hepatocellular carcinoma) as a model were individually incubated with each of the complexes (1  $\mu\text{M}$ ) for 60 min, and then probed under two-photon confocal laser scanning microscopy. The three complexes displayed intense *in cellulo* fluorescence after incubation (Fig. 2 and S11). Intriguingly, the locations of the three complexes in living cells were completely different. While **DTTP-ZnCl<sub>2</sub>** and **DTTP-ZnBr<sub>2</sub>** clearly located at nuclear region, signals from **DTTP-ZnI<sub>2</sub>** apparently exclude from cell nuclear but a generalized cytosolic staining pattern was observed.

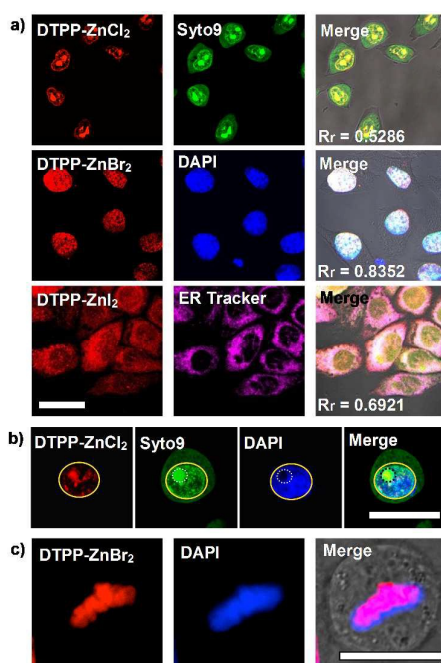


Fig. 2 (a) Two-photon fluorescent images of HepG2 cells treated with **DTTP-ZnX<sub>2</sub>** ( $X = \text{Cl}, \text{Br}$  and  $\text{I}$ ) and the corresponding colocalization dyes. For **DTTP-ZnCl<sub>2</sub>**, **DTTP-ZnBr<sub>2</sub>** and **DTTP-ZnI<sub>2</sub>**, Syto9, DAPI and ER dyes were used, respectively. (b) Two-photon fluorescent images of HepG2 cells treated with **DTTP-ZnCl<sub>2</sub>**, Syto9

and DAPI. (c) Two-photon fluorescent images of dividing HepG2 cells treated with **DTTP-ZnBr<sub>2</sub>** and DAPI. Scale bars = 20  $\mu\text{m}$ .

To precisely determine the subcellular locations of these complexes, HepG2 cells incubated individually with **DTTP-ZnCl<sub>2</sub>**, **DTTP-ZnBr<sub>2</sub>** and **DTTP-ZnI<sub>2</sub>** were co-stained with the commercial organelle probes Syto9 for intracellular RNA (cytosolic and nuclear RNA), 4',6-diamidino-2-phenylindole (DAPI) for nuclear DNA, and lipophilic endoplasmic reticulum tracker (ER tracker), respectively (Fig. 2). In Fig. 2a, **DTTP-ZnCl<sub>2</sub>** displayed a high signal overlap with Syto9 in the nuclear region but not in cytosolic region, and its Pearson's coefficient ( $R_r$ ) was 0.5286, suggesting that **DTTP-ZnCl<sub>2</sub>** is mainly located within nucleoli. Meanwhile, the incubation of HepG2 cells with **DTTP-ZnBr<sub>2</sub>** displayed perfect overlap with DNA-specific DAPI ( $R_r=0.8352$ ), which can evident that intracellular binding sources of **DTTP-ZnBr<sub>2</sub>** is nucleic DNA. In contrast to **DTTP-ZnCl<sub>2</sub>** and **DTTP-ZnBr<sub>2</sub>**, **DTTP-ZnI<sub>2</sub>** exhibited higher level of overlapping with ER tracker, and its Pearson's coefficient was  $R_r = 0.6921$  (Fig. 2a). The relatively lower Pearson's coefficient implied that **DTTP-ZnI<sub>2</sub>** also could be internalized with other membrane-rich organelles, such as mitochondria and Golgi apparatus.

More importantly, as shown in magnified images (Fig. 2b), it is apparently that as **DTTP-ZnCl<sub>2</sub>** preferentially binds to nucleoli over other nuclear substances, since no emission from DAPI was detected from **DTTP-ZnCl<sub>2</sub>** labelled nucleolar region (indicated by white circle). Moreover, during cell dividing in a pre-metaphase cell, for instance, when the nuclear membrane disappeared and nucleoli disassembled (Fig. 2c), the luminescent signal of **DTTP-ZnBr<sub>2</sub>** remained highly colocalized with DAPI, which again strongly implied that the binding sources of **DTTP-ZnBr<sub>2</sub>** in living cells nuclear is DNA (Fig. S13), which also supported by molecular docking results (Fig. S14). The initial two-photon confocal studies indicated the high affinity of these complexes with their correspondence subcellular compartments over another intracellular species. To further confirm the intracellular distributions of the three complexes, transmission electron microscopy (TEM) tests were

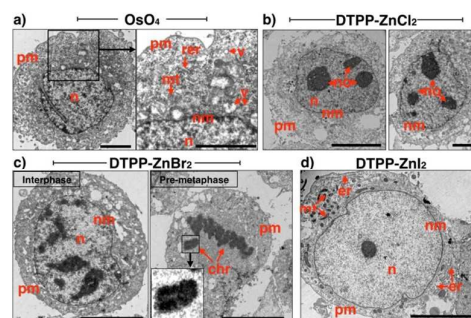


Fig. 3 (a) TEM images of HepG2 treated with  $\text{OsO}_4$  solely as control experiments. (b-d) TEM images of HepG2 treated with **DTTP-ZnCl<sub>2</sub>**, **DTTP-ZnBr<sub>2</sub>** and **DTTP-ZnI<sub>2</sub>**, respectively. Abbreviations: n = nucleus, mt = mitochondria, pm = plasma membrane, nm = nuclear membrane, no = nucleolu, v = vesicles, er = endoplasmic reticulum,

rer = rough endoplasmic reticulum, chr = chromosomes. Scale bar = 5  $\mu$ m.

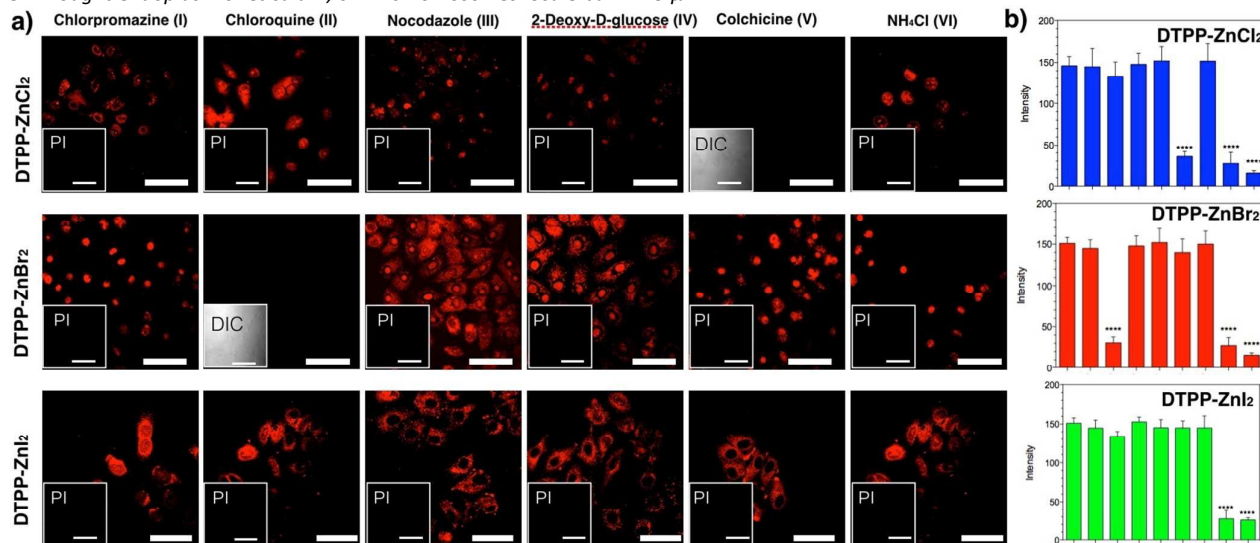


Fig. 4 (a) Treatment with the cell entry inhibitors show uptake of **DTTP-ZnCl<sub>2</sub>** (upper), **DTTP-ZnBr<sub>2</sub>** (central) and **DTTP-ZnI<sub>2</sub>** (lower) by HepG2 cells, while propidium iodide (PI) indicated the cell mortality after treatments. (b) Relative fluorescence intensities of cells treated with **DTTP-ZnCl<sub>2</sub>** (left), **DTTP-ZnBr<sub>2</sub>** (middle) and **DTTP-ZnI<sub>2</sub>** (right). Scale bars = 50  $\mu$ m.

performed using these three complexes as contrast agents<sup>[31]</sup> (Fig. 3). We firstly used osmium tetroxide (OsO<sub>4</sub>) incubating cells as control experiments to enhance the membrane contrast. As shown in left column of Fig. 3a, positive control cells were stained solely with OsO<sub>4</sub>, a phospholipid contrast agent that widely used in TEM, and their intracellular membrane structures including mitochondria, vesicles, and rough endoplasmic reticulum, plasma membrane and nuclear membrane were clearly observed in magnified picture. When HepG2 cells incubated with **DTTP-ZnCl<sub>2</sub>** without OsO<sub>4</sub>, intracellular membrane compartments presented negligible signal, whereas two representative micrographs showed much better contrast in cell nucleolus due to the accumulation of **DTTP-ZnCl<sub>2</sub>** (Fig. 3b). In the case of **DTTP-ZnBr<sub>2</sub>**, it was found that nuclear region beard much higher concentration in an interphase cell, and **DTTP-ZnBr<sub>2</sub>** clearly localizes within chromatin (Fig. 3c, left). It was also interesting to note that in a pre-metaphase cell, once the nuclear membrane disappeared, consistent **DTTP-ZnBr<sub>2</sub>** signal was observed from DNA dense chromosomes (Fig. 3c, right) and displayed typical chromosomal quaternary tubular structure. On the contrary, when HepG2 cells were incubated with **DTTP-ZnI<sub>2</sub>**, much less nuclear uptake occurred with a clear presentation of the intracellular membrane compartments including ER, mitochondria, vesicles and nuclear membrane. The above TEM studies are in well agreement with the initial cell staining results exploited under confocal microscopy; further strengthen those complexes **DTTP-ZnCl<sub>2</sub>**, **DTTP-ZnBr<sub>2</sub>** and **DTTP-ZnI<sub>2</sub>** targeted different subcellular compartments, although the three complexes share similar structural apart from the coordinate halide moiety.

To seek the reasonable explanation for this intriguing phenomenon, cell uptake mechanisms of **DTTP-ZnCl<sub>2</sub>**, **DTTP-ZnBr<sub>2</sub>** and **DTTP-ZnI<sub>2</sub>** were investigated under different incubation temperatures (0 and 25 °C) and *via* inhibition studies using well-documented endocytosis and active transport inhibitors.<sup>[32, 33]</sup> According to the results as shown in Fig. 4a and 4b, we proposed the uptake mechanisms: the three complexes entered cells via different energy-dependent uptake mechanisms; where **DTTP-ZnCl<sub>2</sub>** via classic endocytosis, **DTTP-ZnBr<sub>2</sub>** via active transport, and **DTTP-ZnI<sub>2</sub>** via a non-endocytotic/non-active transport, but energy dependent pathway. As a result, complexes **DTTP-ZnCl<sub>2</sub>**, **DTTP-ZnBr<sub>2</sub>** and **DTTP-ZnI<sub>2</sub>** penetrated through the plasma/nuclear membrane and accumulated to a great extent within nucleoli, nucleus and other intercellular membrane system, respectively. It is noteworthy that endocytotic mechanism might also partially involved in taking up **DTTP-ZnBr<sub>2</sub>** in living cells, as nocodazole, 2-deoxy-D-glucose and colchicine obviously influenced the intracellular diffusion and caused unspecific cytosolic fluorescence. Above proposed cell entry mechanisms were further supported using pre-fixed and permeabilized cells. Once membrane proteins lost their functions due to the fixation, these complexes displayed non-specificity towards nucleoli, nucleus and endoplasmic reticulum (Fig. S16 and S17), and a generalized whole cell-staining pattern was also observed. These results indicated that the coordinated halide anions significantly influence the cell entry pathway, leading to different localizations in living cells. It is noted that the three complexes may be not very stable in actual biological environments, since there are a large number of bio-molecules in living cells, including thiols, amino acids, various anions and others species. In this study, we mixed the

complexes and various biological species, and measured their fluorescent responses. As shown in Fig. S18, most of biomolecules except  $\text{HS}^-$  and  $\text{PO}_4^{3-}$  cannot influence the emission of the three complexes. Although  $\text{HS}^-$  and  $\text{PO}_4^{3-}$  could substitute **DTPP**, the disassociated **DTPP** not emits two-photon signal, thus the substitution would not interfere two-photon fluorescent imaging in desired targeting sub-cellular organelles. Moreover, widespread  $\text{Cl}^-$  in bio-environment easily lead to anion exchanges with  $\text{Br}^-$  and  $\text{I}^-$ , when the complexes existed as monomer state in solution as shown in Fig. S19. However, the three hydrophobic complexes cannot dissolve in bio-environmental aqueous solution with large amounts of  $\text{Cl}^-$ , but rather existed as nanoparticles. As shown in Fig. S20, the sizes of Cl, Br, and I complexes were  $\sim 30$ , 50, 1000 nm, respectively. Importantly, the formations of nanoparticles largely decreased the rate of anion exchanges (Fig. S21), and the difference of nanoparticles sizes induced the different cellular uptake mechanisms.

In summary, we have present three terpyridine deviations zinc-halide complexes with two-photon fluorescence, and demonstrated how the complexes successfully rerouted and specifically target different subcellular organelles in live cells by tuning coordination anions ( $\text{Cl}^-$ ,  $\text{Br}^-$  and  $\text{I}^-$ ). By hijacking individual entry mechanism, complex **DTPP-ZnCl<sub>2</sub>** targets nucleoli, **DTPP-ZnBr<sub>2</sub>** binds to nuclear DNA and **DTPP-ZnI<sub>2</sub>** shows cytosolic membranous compartments uptake. Our results introduced a concept that could have significant implications and potentials in utilizing such complexes as biomolecular transporter.

This work was supported by a grant for the National Natural Science Foundation of China (21602003, 51372003, 21271004, 51432001, and 51271003, 21501001), Anhui University Doctor Startup Fund (J01001962). The work of molecular modeling calculations on Discovery Studio (Dassault Systemes BIOVIA, Discovery Studio Modeling Environment, Release 4.5, San Diego: Dassault Systemes, 2015) was contributed by Professor Aidong Wang from Huangshan University, China.

## Notes and references

- [1] H. F. Lodish, A. Berk, S. L. Zipursky, P. Matsudaira, D. Baltimore, J. Darnell, *Molecular cell biology, Citeseer*, Vol. 4.
- [2] W. Denk, J. H. Strickler, W.W. Webb, *Science*, **1990**, 248, 73-76.
- [3] W. R. Zipfel, R. W. Williams, W. W. Webb, *Nat. Biotechnol.*, **2003**, 21, 1369-1377.
- [4] R. W. Williams, W. R. Zipfel, W. W. Webb, *Curr. Opin. Chem. Boil.*, **2001**, 5, 603-608.
- [5] F. Helmchen, W. Denk, *Nat. Methods.*, **2005**, 2, 932-940
- [6] H. B. Kim, B. R. Cho, *Chem. Rev.* **2015**, 115, 5014-5055.
- [7] M. P. Murphy, R. A. J. Smith. *Annu. Rev. Pharmacol. Toxicol.*, **2007**, 47, 629-656.
- [8] L. F. Yousif, K. M. Stewart, S. O. Kelley, *ChemBioChem*, **2009**, 10, 1939-1950.
- [9] a) Q. Q. Wan, S. M. Chen, W. Shi, L. H. Li, H. M. Ma, *Angew. Chem. Int. Edit.*, **2014**, 53, 10916-10920.
- [10] M. Gao, Q. L. Hu, G. X. Feng, B. Z. Tang, B. Liu, *J. Mater. Chem. B*, **2014**, 2, 3438-3442.
- [11] B. G. Wang, S. C. Yu, X. Y. Chai, T. J. Li, Q. Y. Wu, T. Wang, *Chem-Eur. J.*, **2016**, 22, 5649-5656.
- [12] a) E. Baggaley, J. A. Weinstein, J. G. Williams, *Coordin Chem. Rev.*, **2012**, 256, 1762-1785.
- [13] Q. Zhao, C. H. Huang, F. Y. Li, *Chem. Soc. Rev.*, **2011**, 40, 2508-2524.
- [14] F. Tessore, D. Roberto, R. Ugo, M. Pizzotti, S. Quici, M. Cavazzini, S. Bruni, F. De Angelis, *Inorg. Chem.*, **2005**, 44, 8967-8978.
- [15] S. Petoud, S. M. Cohen, J. C. G. Bünzli, K. N. Raymond, *J. Am. Chem. Soc.*, **2003**, 125, 13324-13325.
- [16] J. Zhang, Y. Liu, Y. Li, H. X. Zhao, X. H. Wan, *Angew. Chem. Int. Ed.* **2012**, 51, 4598-4602.
- [17] W. Sun, J. B. Yu, R. P. Deng, Y. Rong, B. Fujimoto, C. F. Wu, H. J. Zhang, D. T. Chiu, *Angew. Chem. Int. Ed.* **2013**, 52, 11294-11297.
- [18] a) J. Tang, Y. B. Cai, J. Jing, J. L. Zhang, *Chem. Sci.*, **2015**, 6, 2389-2397.
- [19] D. Xie, J. Jing, Y. B. Cai, J. Tang, J. J. Chen, J. L. Zhang, *Chem. Sci.*, **2014**, 5, 2318-2327.
- [20] J. Jing; J. J. Chen; Y. Hai, J. Zhan, P. Xu, J. L. Zhang, *Chem. Sci.*, **2012**, 3, 3315-3320.
- [21] a) C.C. Liaw, W. Y. Liao, C. S. Chen, S. C. Jao, Y. C. Wu, C. N. Shen, S. H. Wu, *Angew. Chem. Int. Ed.* **2011**, 50, 7885-7891.
- [22] H. Dau, M. Haumann, *Coordin Chem. Rev.*, **2008**, 252, 273-295.
- [23] P. F. Wang, Z. R. Hong, Z. Y. Xie, S. W. Tong, O. Y. Wong, C. S. Lee, N. B. Wong, L. S. Hung, S. T. Lee, *Chem. Commun.*, **2003**, 14, 1664-1665.
- [24] a) S.J. Stohs, D. Bagchi, *Free Radical Bio. Med.*, **1995**, 18, 321-336.
- [25] K. P. Carter, A. M. Young, A. E. Palmer, *Chem. Rev.*, **2014**, 114, 4564-4601.
- [26] a) J. Tang, J. J. Chen, J. Jing, J. Z. Chen, H. Lv, Y. Yu, P. Xu, J. L. Zhang, *Chem. Sci.*, **2014**, 5, 558-566.
- [27] J. P. Holland, F. I. Aigbirhio, H. M. Betts, P. D. Bonnitche, P. Burke, M. Christlieb, G. C. Churchill, A. R. Cowley, J. R. Dilworth, P. S. Donnelly, *Inorg. Chem.* **2007**, 46, 465-485.
- [28] Y. You, E. Tomat, K. Hwang, T. Atanasijevic, W. Nam, A. P. Jasanoff, S. J. Lippard, *Chem. Comm.* **2010**, 46, 4139-4141.
- [29] S. Bhowmik, B. N. Ghosh, V. Marjomäki, K. Rissanen, *J. Am. Chem. Soc.*, **2014**, 136, 5543-5546.
- [30] G. Bort, T. Gallavardin, D. Ogden, P. I. Dalko, *Angew. Chem. Int. Edit.*, **2013**, 52, 4526-4537.
- [31] X. H. Tian, Q. Zhang, M. Z. Zhang, K. Uvdal, Q. Wang, J. Y. Chen, W. Du, B. Huang, J. Y. Wu, Y. P. Tian, *Chem. Sci.*, **2017**, 8, 142-149.
- [32] H. K. Ziegler and E. R. Unanue, *Proc. Natl. Acad. Sci. U. S. A.*, **1982**, 79, 175-178.
- [33] C. A. Puckett and J. K. Barton, *Biochemistry*, **2008**, 47, 11711-11716.